Competing anisotropies and temperature dependence of exchange bias in Co|IrMn metallic wire arrays fabricated by nanoimprint lithography

Wei Zhang,[1,a)] Dirk N. Weiss,[2] and Kannan M. Krishnan[1,b)]
[1]*Materials Science and Engineering, University of Washington, Seattle, Washington 98105, USA*
[2]*Washington Technology Center, Seattle, Washington 98195-0001, USA*

(Presented 19 January 2010; received 28 October 2009; accepted 10 December 2009; published online 7 May 2010)

The magnetic behavior of exchange biased Co|IrMn bilayer metallic wire arrays, fabricated by nanoimprint lithography, was studied and compared with identical thin film heterostructures. A significant uniaxial shape anisotropy, $K_{U\text{-shape}}$, in addition to the unidirectional exchange anisotropy, K_E, and the intrinsic uniaxial anisotropy, $K_{U\text{-intrinsic}}$ observed in the unpatterned film, was introduced in the wire arrays through wire patterning. The competing anisotropies were shown to modify the angular dependence of exchange bias, H_{EB}, and coercivity, H_C, for wire arrays. In addition, an asymmetric behavior is observed for both wire arrays and unpatterned film and is attributed to the noncollinear alignment of uniaxial and unidirectional anisotropies. Temperature dependence of H_{EB} is different for the wire arrays from the unpatterned thin film. This and the large deviation from ideal cubic anisotropy in the antiferromagnet for the wire arrays are both in agreement with Malozemoff's model of exchange bias. © *2010 American Institute of Physics*. [doi:10.1063/1.3367959]

I. INTRODUCTION

The shift of the hysteresis loop of a ferromagnet (F) in direct contact to an antiferromagnet (AF) when cooled in an external field through the Néel temperature of the AF is termed as exchange bias (EB).[1] Intuitively, in EB, uncompensated AF spins at the F|AF interface couple with F spins and, if the former are pinned, give rise to an additional unidirectional anisotropy, K_E, in the F. For thin films, this anisotropy can either be in plane[2] or out of plane.[3] However, if the uncompensated AF spins are not pinned, they only add resistance to the magnetic reversal,[4] resulting in an enhancement of coercivity, H_C. Another related feature of EB is the asymmetry in the magnetization reversal[5–7] behavior. From a technological point of view, many applications require tailoring of the above properties with emphasis on controlling the different magnetic anisotropies. Specifically, the magnetostatic or shape anisotropy, K_{MS}, can be controlled by patterning the sample into uniform arrays of nanostructured elements.[8,9] For elements with large aspect ratios, such as wires, the shape anisotropy is uniaxial, or $K_{MS}=K_{U\text{-shape}}$. Fabrication of such nanostructured elements by conventional optical and electron-beam lithography techniques is resolution limited and too time consuming in making large area arrays, respectively. On the other hand, recently developed nanoimprint lithography (NIL) methods,[10] capable of large-area patterning with high throughput and resolution, are promising for patterning arrays of interest in magnetism.[11] In this context, we report on the role of competing anisotropies and the temperature dependence of EB in Co|IrMn (F|AF) samples prepared as a continuous film sample (S_{film}) and NIL-patterned metallic wire arrays (S_{wire}). We show that the relative magnitudes of the competing anisotropies K_U—introduced through wire patterning—and the unidirectional exchange anisotropy, K_E, as well as their relative orientations influence the angular dependence of the magnetization behavior. Further, the temperature dependence of EB is different for S_{film} and S_{wire}; this is explained in terms of Malozemoff's model[12] of EB.

II. EXPERIMENT

We fabricated arrays of approximately 400 nm wide metallic wires using a Nanonex NXB-100 nanoimprinter, a grating mold (Lightsmyth Inc.) with 12.5×12.5 mm^2 patterned area, and a bilayer lift-off recipe described in Ref. 11, see also Figs. 1(a)–1(d). A bilayer resist template (quasi-one-dimensional lines) with undercut profile was produced by

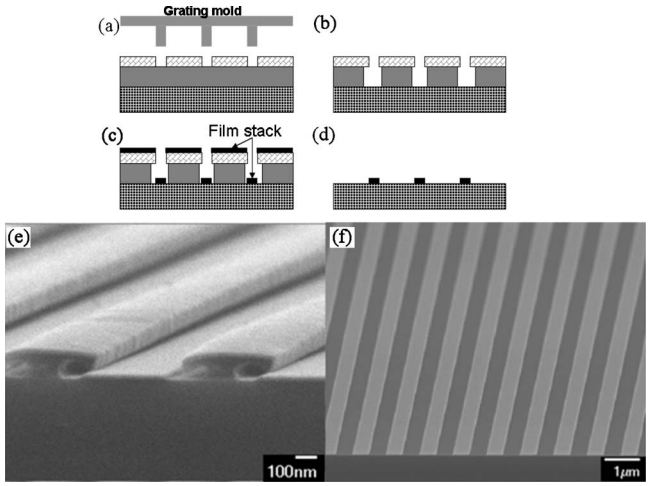

FIG. 1. (a)–(d) Schematic illustration of Co|IrMn exchange biased wire arrays fabricated by bilayer NIL. (e) Metal deposited on bilayer resist undercut profile (SEM micrograph). (f) Exchange biased, polycrystalline, Co|IrMn wire arrays obtained after resist lift-off (SEM micrograph).

a)Electronic mail: zwei@u.washington.edu.
b)Author to whom correspondence should be addressed. Electronic mail: kannanmk@u.washington.edu.

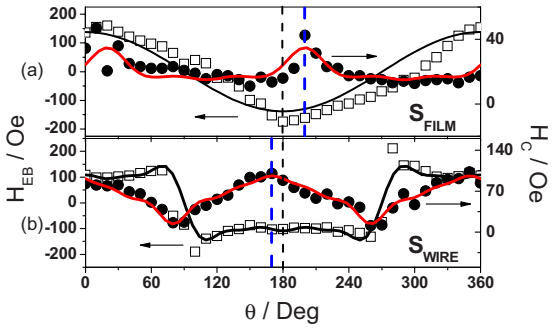

FIG. 2. (Color online) Angular dependence of coercivity and EB field of annealed sample (a) S_{film} and (b) S_{wire}. All curves fitted to Ambrose's model. Thin dashed line indicates the K_E direction, at 180°; thick dashed line indicates the coercivity peaks.

imprinting and subsequently etching the upper layer [Fig. 1(a)], and selectively developing the bottom layer [Fig. 1(b)]. Metal multilayer films were deposited by ion beam sputtering, Fig. 1(c), followed by a final resist lift-off, Fig. 1(d). A series of metal multilayer lines, with the sequence Cu(5 nm)/Co(5 nm)/IrMn(10 nm)/Pt(2 nm), was deposited. A permanent magnet with magnetization direction parallel to the metal lines was placed on the back of all the substrates, during thin film growth, to induce and control the EB direction. Scanning electron microscopy (SEM) images show the resist undercut profile [Fig. 1(e)] and the final patterned wires displaying very good resolution and uniformity [Fig. 1(f)]. The uniaxial magnetic shape anisotropy along the line direction is determined by the wire morphology. Exchange anisotropy is established by placing a permanent magnet parallel to the wire direction (shape anisotropy) during film growth. As a control, a Co|IrMn continuous film sample, S_{film}, was also grown with the same multilayer architecture. Each as-grown sample was cut into many small pieces for selective postgrowth treatment. Several film and wire pieces were subsequently annealed in a vacuum chamber for 1 h at 280 °C, with a permanent magnet positioned along the same direction as the growth, and others kept in their as-grown state. Magnetic properties were measured at room temperature (RT) by magneto-optic Kerr effect (MOKE) and as a function of temperature (20–480 K) using a physical property measurement system (Quantum Design).

III. RESULTS AND DISCUSSION

The angular dependence of the coercivity, $H_C(\theta)$, and the EB field, $H_{EB}(\theta)$, were measured by MOKE at RT for annealed samples, S_{film} and S_{wire} [Figs. 2(a) and 2(b)]. For analysis, we applied the model of Ambrose *et al.*,[13] asserting that the unidirectional anisotropy has an inherent symmetry of $UD(\pi+\phi)=-UD(\phi)$ and uniaxial anisotropy has an inherent symmetry of $UA(\pi+\phi)=UA(\phi)$, resulting in the basic symmetry properties of H_C and H_{EB},

$$H_C(\theta) = H_C(0) \sum_{n=\text{even}} b_n \cos(n\theta), \tag{1a}$$

$$H_{EB}(\theta) = H_{EB}(0) \sum_{n=\text{odd}} b_n \cos(n\theta), \tag{1b}$$

where ϕ is the angle between the magnetization and exchange anisotropy axis and θ is the angle between the applied field and the EB direction, i.e., $\theta=0°$ represents the direction of K_E. H_{EB} for S_{film} is reproduced by a single *cosine* term and expressed as $H_{EB}(\theta)=138$ Oe $\cos\theta$ (higher order terms are negligible). The angular dependence of coercivity, $H_C(\theta)$, displays two peaks; however, both are shifted to higher angles, by about 20°, with respect to 0° and 180°. The data points around 0° have large experimental errors due to the weak MOKE signals (around 0°) with the ensuing inaccurate reading of switching fields from hysteresis loops, but the 20° shift is clearly seen at $\theta=200°$ (=180°+20°). This shift indicates the existence of a small uniaxial anisotropy at an angle of 20° from the direction of K_E. This uniaxial anisotropy, termed as $K_{U\text{-intrinsic}}$, is very likely caused by the oblique growth condition during deposition, as the ion beam is directed from the target to the substrate at a small angle.[14] Taking into account the misalignment of the $K_{U\text{-intrinsic}}$ and K_E, the angular dependence of coercivity can be well fitted, without including the noisy data around 0°, by even cosine terms expressed as $H_C(\theta)=20$ Oe $[1+0.34\cos 2(\theta-20°)-0.2\cos 4(\theta-20°)+0.14\cos 6(\theta-20°)-0.02\cos 8(\theta-20°)+0.01\cos 10(\theta-20°)]$. Further, a small asymmetric behavior was observed for H_{EB}, which is also attributed to the misalignment of K_E and $K_{U\text{-intrinsic}}$.

For the S_{wire} sample, due to the additional uniaxial shape anisotropy $K_{U\text{-shape}}$, arising from the wire morphology, the angular behaviors of H_{EB} and H_C are both greatly modified. The coercivity was largely enhanced and clearly exhibited two maxima at ≈170° and ≈350° and two minima at ≈80° and ≈260°. The angular dependence of coercivity satisfies $H_C(\theta)=63$ Oe $[1+0.5\cos 2(\theta+10°)-0.07\cos 4(\theta+10°)+0.1\cos 6(\theta+10°)-0.05\cos 8(\theta+10°)+0.05\cos 10(\theta+10°)]$. The peaks of $H_C(\theta)$ are shifted to lower angle with respect to K_E, by ~−10°, indicating that the effective K_U, combining $K_{U\text{-intrinsic}}$ and $K_{U\text{-shape}}$, is noncollinear by about −10° with respect to K_E. From these measurements, $K_{U\text{-intrinsic}}$ and $K_{U\text{-shape}}$ cannot be determined individually. For EB, a single cosine term is no longer enough for fitting $H_{EB}(\theta)$; higher order cosine terms are required to obtain a good fitting, i.e., $H_{EB}(\theta)=136$ Oe $(\cos\theta-0.42\cos 3\theta+0.28\cos 5\theta-0.13\cos 7\theta+0.08\cos 9\theta)$. Besides, two asymmetric points are observed in $H_{EB}(\theta)$, at $\theta=100°$ and $\theta=280°$. The higher order terms in the fitting and the asymmetric points in $H_{EB}(\theta)$ are both attributed to the wire-induced shape anisotropy along with the misalignment of K_E and effective K_U in the S_{wire} sample.

The temperature dependence of H_{EB} and H_C were also studied. Hysteresis loops were measured systematically along the bias direction over a broad temperature range from 20–480 K. The temperature dependences, $H_C(T)$ and $H_{EB}(T)$, for S_{wire} and S_{film} are summarized and shown in Fig. 3. The blocking temperature, T_B, is determined to be ~440 K for both S_{wire} and S_{film}, indicating an insignificant finite-size effect.[15] The overall coercivity of S_{wire} is greatly enhanced compared to S_{film} due to the added shape uniaxial anisotropy.

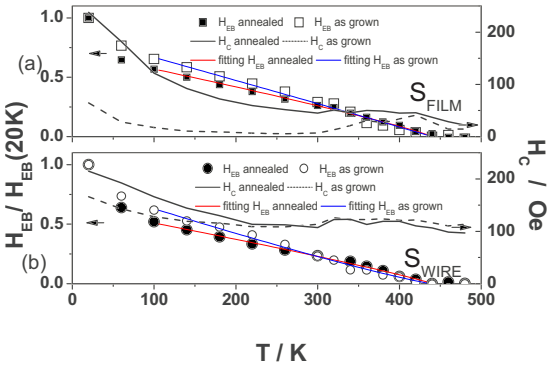

FIG. 3. (Color online) Temperature dependence of H_C and H_{EB} for (a) S_{film} and (b) S_{wire}. $H_{EB}(T)$ data are fitted to the Malozemoff model within the linear region, from 100 K to T_B. Fitting parameters are summarized in Table I.

For both samples, especially for S_{film}, postannealing the sample leads to a significant increase of coercivity, at $20 < T < \sim 300$ K; however, this annealing effect is not observed for $RT < T < T_B$, for both samples, in Figs. 3(a) and 3(b). We propose that this is because the two components contributing to the coercivity, i.e., magnetocrystalline anisotropy of the F layer and interfacial unpinned AF spins,[16] dominate in different temperature regimes. In the low temperature range (from 20 to ~300 K), where the magnetocrystalline anisotropy of the F layer dominates, significant coercivity enhancement by annealing is observed, along with an increase in saturation magnetization.[17] However, in the higher temperature range (~RT to T_B) where the unpinned AF spins dominate, a coercivity enhancement is observed around T_B (Ref. 18) and the annealing effect is relatively insignificant since the density of unpinned AF spins is not sensitive to the annealing.

An increase in H_{EB} after annealing for both S_{film} and S_{wire} is observed and this is attributed to an increased F|AF pinning at the interface.[19] To further investigate the behavior, $H_{EB}(T)$ is normalized with respect to H_{EB} measured at the lowest temperature (20 K) and the decay of the pinned biasing fraction of AF spins is plotted independent of their absolute numbers. At the temperature range between 100 K and T_B, $H_{EB}(T)$ shows good agreement with Malozemoff's theory[12] with modified exponent, γ,

$$H_{EB}(T)/H_{EB}(20\ \mathrm{K}) = A\left(1 - \frac{T}{T_B}\right)^{\gamma}, \qquad (2)$$

where the exponent $\gamma=1$ for cubic antiferromagnetic anisotropy. Deviations from $\gamma=1$ have been reported for various EB systems and are thought to be a good measure of the antiferromagnetic ordering.[20] The fitting parameters for our samples are listed in Table I.

$\gamma=0.99$ for as-grown S_{film} sample, indicating a very good cubic anisotropy and $\gamma=1.14$ for as-grown S_{wire}, which deviates from cubic anisotropy and is attributed to the increased amount of disordered atomic arrangement and the lowering of symmetry caused by the reduced dimensions of the wires. For annealed samples, γ is greatly reduced for both, i.e., $\gamma=0.88$ for S_{film} and $\gamma=0.89$ for S_{wire}, indicating similar temperature behavior of the pinned AF spins due to the modified interface structures after annealing. Similar $H_{EB}(T)$ behaviors, reported recently for as-grown and annealed samples, were associated with changes in interface structure, i.e., increased interface roughness, which serves as pinning centers for the ferromagnetic layer and can dramatically enhance both EB and coercivity.[19] At the temperature range below 100 K, $H_{EB}(T)$ follows a behavior much like an exponential decay, which has also been found in Refs. 19 and 21 and is in good agreement with theoretical simulations.[22]

TABLE I. Fitting parameters for as-grown and annealed sample S_{film} and S_{wire} according to Eq. (2).

	S_{film}		S_{wire}	
	As grown	Annealed	As grown	Annealed
A	0.86	0.71	0.84	0.64
γ	0.99	0.88	1.14	0.89

ACKNOWLEDGMENTS

This work was supported by DoE/BES under Grant No. ER45987. D.N.W. also acknowledges DARPA (Grant No. N66001–06–1–2017) funding for development of nanoimprint lithography.

[1] W. H. Meiklejohn and C. P. Bean, Phys. Rev. **102**, 1413 (1956); **105**, 904 (1957).
[2] S. Roy, M. R. Fitzsimmons, S. Park, M. Dorn, O. Petracic, I. V. Roshchin, Z.-P. Li, X. Batlle, R. Morales, A. Misra, X. Zhang, K. Chesnel, J. B. Kortright, S. K. Sinha, and I. K. Schuller, Phys. Rev. Lett. **95**, 047201 (2005).
[3] X. Ji and K. M. Krishnan, J. Appl. Phys. **99**, 08C105 (2006); X. Ji, A. B. Pakhomov, and K. M. Krishnan, *ibid.* **101**, 09E507 (2007).
[4] M. D. Stiles and R. D. McMichael, Phys. Rev. B **63**, 064405 (2001).
[5] M. R. Fitzsimmons, P. Yashar, C. Leighton, I. K. Schuller, J. Nogués, C. F. Majkrzak, and J. A. Dura, Phys. Rev. Lett. **84**, 3986 (2000).
[6] K.-U. Barholz and R. Mattheis, J. Appl. Phys. **91**, 7224 (2002).
[7] P. Blomqvist, K. M. Krishnan, and H. Ohldag, Phys. Rev. Lett. **94**, 107203 (2005).
[8] J. Nogués, J. Sort, V. Langlais, V. Skumryev, S. Surinach, J. S. Munoz, and M. D. Baró, Phys. Rep. **65**, 422 (2005).
[9] K. M. Krishnan, A. B. Pakhomov, Y. Bao, P. Blomqvist, Y. Chun, M. Gonzales, K. Griffin, X. Ji, and B. K. Roberts, J. Mater. Sci. **41**, 793 (2006).
[10] S. Y. Chou, P. R. Krauss, and P. J. Renstrom, J. Vac. Sci. Technol. B **14**, 4129 (1996).
[11] W. Hu, R. J. Wilson, L. Xu, S.-J. Han, and S. X. Wang, J. Vac. Sci. Technol. A **25**, 1294 (2007).
[12] A. P. Malozemoff, J. Appl. Phys. **63**, 3874 (1988).
[13] T. Ambrose, R. L. Sommer, and C. L. Chien, Phys. Rev. B **56**, 83 (1997).
[14] Q. F. Zhan, C. V. Haesendonck, S. Vandezande, and K. Temst, Appl. Phys. Lett. **94**, 042504 (2009).
[15] L. Sun, P. C. Searson, and C. L. Chien, Phys. Rev. B **61**, R6463 (2000).
[16] S. Brück, E. Goering, G. Schutz, X. Ji, and K. M. Krishnan, Phys. Rev. Lett. **101**, 126402 (2008).
[17] J. Huang, L. He, Y. Leng, W. Zhang, X. Li, C. Chen, and Y. Liu, Nanotechnology **18**, 415603 (2007).
[18] W. Pan, N.-Y. Jih, C.-C. Kuo, and M.-T. Lin, J. Appl. Phys. **95**, 7297 (2004).
[19] G. Nowak, A. Remhof, F. Radu, A. Nefedov, H.-W. Becker, and H. Zabel, Phys. Rev. B **75**, 174405 (2007).
[20] N. N. Phuoc and T. Suzuki, IEEE Trans. Magn. **43**, 897 (2007).
[21] S. G. Wang, A. Kohn, C. Wang, A. K. Petford-Long, S. Lee, R. Fan, J. P. Goff, L. J. Singh, Z. H. Barber, and R. C. C. Ward, J. Phys. D **42**, 225001 (2009).
[22] J.-G. Hu, G. Jin, A. Hu, and Y. Ma, Eur. Phys. J. B **40**, 265 (2004).